

## Reduced conductivity in the terahertz skin-depth layer of metals

N. Laman and D. Grischkowsky<sup>a)</sup>

*School of Electrical and Computer Engineering, Oklahoma State University, Stillwater, Oklahoma 74078*

(Received 26 January 2007; accepted 16 February 2007; published online 23 March 2007)

The terahertz conductivities of plates of Cu and Al were measured to remain the same at 295 and 77 K using waveguide terahertz time domain spectroscopy (THz-TDS). This result was true for a variety of commercial alloys and surface preparations. Consequently, carrier scattering by lattice defects within the 100 nm THz skin depth is much larger than scattering by phonons at room temperature. However, an exception was found to be the THz skin-depth layer of an evaporated 300 nm Al film in contact with a polished Si surface. For this interface Al layer, the conductivity increased by a factor of 4 when cooled to 77 K. © 2007 American Institute of Physics. [DOI: 10.1063/1.2716066]

The metal parallel plate waveguide has been demonstrated to be an outstanding THz interconnect with low loss and very low group velocity dispersion. The measured performance of the THz single mode metal waveguides,<sup>1</sup> and the THz transverse electromagnetic (TEM) mode metal parallel plate waveguides<sup>2,3</sup> has been limited by the metal conductivity. Consequently, in order to further improve performance, the metal conductivity must be increased. A simple and effective method to increase conductivity has been to cool metals to liquid nitrogen temperatures.<sup>4,5</sup> Not only can one potentially use this technique to increase the throughput of the waveguides. A careful observation of the waveguide performance can also yield a measurement of the frequency dependent conductivity.

The experimental setup to test cooling the waveguide is similar to that of the first demonstration of single TEM mode THz pulse propagation through a metal parallel plate waveguide.<sup>2</sup> Here, however, the waveguide assembly is a complete unit with metal lens holders (attached to the waveguide) enabling the stable alignment of the high resistivity cylindrical Si lenses in contact with the input and output faces of the waveguide. This assembly is placed in a vacuum chamber with straight through optical access positioned in the center of the standard THz-TDS system.<sup>6</sup> For our case the chamber has a liquid nitrogen container in contact with the waveguide assembly.<sup>7</sup>

In order to monitor the effects of the pump laser drift, the THz signal through the waveguide as well as the signal of another THz-TDS system operating with the same laser are continuously measured during the cooldown and subsequent warmup of the waveguide assembly. The temperature of the waveguide is monitored by measuring the change of the temporal delay due to the temperature dependent refractive index of the Si ( $dn/dT=1.3 \times 10^{-4}/\text{K}$ ).<sup>8</sup> The cumulative, relative change between room temperature at 295 K and liquid nitrogen temperature at 77 K in the refractive index ( $\Delta n/n=-8.5 \times 10^{-3}$ ) is the dominant effect since it is much larger than the corresponding change in the length of the silicon ( $\Delta L/L=-0.23 \times 10^{-3}$ ) (Ref. 9) due to the linear thermal expansion coefficient. All results were confirmed over multiple thermal cycles.

The experiments were first performed on a number of parallel plate waveguides constructed of bulk copper and aluminum. Surprisingly, these waveguides did not show an increase in conductivity upon reducing the temperature from room temperature 295 to 77 K. This was true for a variety of commercial alloys (including Al alloy 1100, Cu alloy 101, and both Al and Cu foils) and surface preparation including fine machining, polishing to an optical finish, and a later etching of these surfaces. Annealed high purity plates (99.99% soft-tempered Al) gave the same results, as did evaporated Al films on an Al substrate. Our conclusion is that for our large class of samples, within the extremely thin approximately 100 nm surface layer (skin depth) penetrated by the propagating THz pulses, the metal plates have so many lattice imperfections that reducing the phonon scattering of electrons by temperature has little effect. This reduction in the realizable THz conductivity due to lattice imperfections caused by ordinary processing techniques could potentially impact proposed THz applications. The majority of the work was performed on Al in order to avoid potential difficulties with the reduction of conductivity at higher frequencies and the anomalous skin effect,<sup>10</sup> both of which would be magnified by copper's relatively long electron scattering time at low temperatures.

In a different approach, we have deposited via e-beam a 300 nm aluminum film on top of a 60 nm titanium adhesion layer first deposited on one surface of a polished Si wafer. The plates of the corresponding metal parallel plate waveguide for this experiment were diced out of this wafer, and the metallic Al surfaces formed the waveguide. Two single-side metal coated Si plates separated by a 50  $\mu\text{m}$  thick spacer were used, and the THz was coupled between the air-spaced plates in the usual manner. Even for these high quality Al films, there was no measurable increase in the conductivity at 77 K. This was repeated for Al films both thermally evaporated and deposited by e-beam onto glass plates, with the same result.

However, a strong increase is seen when the terahertz is coupled through a waveguide comprised of a custom-fabricated 50  $\mu\text{m}$  thick high resistivity Si wafer coated on both sides by thermal evaporation with a 300 nm Al film. This implies that while the Al at the top of the layer (i.e., near the Al/air interface) still has a large number of defects, the Al at the bottom of the layer (i.e., near the Si/Al interface) is relatively defect free. This experimental fact could

<sup>a)</sup>Electronic mail: grischd@ceat.okstate.edu

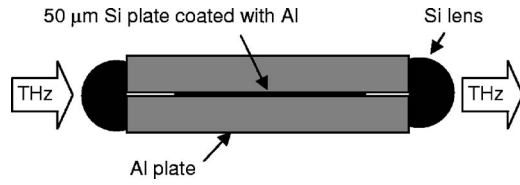


FIG. 1. THz waveguide assembly with Si plate insert.

have technological implications as planar interconnects are extended to increasingly higher frequencies. As shown in Fig. 1, the 30 mm long, Al parallel plate waveguide with plate separation  $b=50\ \mu\text{m}$  contains the precisely diced high resistivity Si plate, 20.0 mm long  $\times$  15.0 mm wide  $\times$  50  $\mu\text{m}$  thick with Al coated planar surfaces. The diced edges are uncoated.

The THz pulses transmitted through the waveguide assembly of Fig. 1 and their corresponding amplitude spectrum are shown in Fig. 2. The pulse at 295 K is the average of 29 scans, resulting in a signal to noise ratio (S/N) of  $\sim 100$ , while the pulse at 77 K is the average of 55 scans, resulting in a S/N of  $\sim 200$ . The amplitude spectrum is the Fourier transform of the full scan length of 16.6 ps. The transmitted terahertz increases considerably at 77 K, particularly at higher frequencies. The 2.96 ps shift to earlier times is due to the index of refraction of the Si decreasing with temperature and agrees with the  $3.2\pm 0.3$  ps theoretical prediction.<sup>8</sup> The total length of cooled Si (two lenses+plate) is 33.1 mm.

The waveguide amplitude absorption coefficients determined by the THz skin-depth layer at the Al/Si interface at 295 and at 77 K are shown in Fig. 3. The absorption coefficient at 295 K is determined by comparing the transmission of the Al waveguide with and without the double-side Al coated Si wafer. The TEM mode Fresnel transmission  $t_{12}t_{21}$  for the two faces of the Si plate within the waveguide is the same as for free space, where  $t_{12}t_{21}=4n/(1+n)^2$  and  $n=3.42$  is the essentially frequency independent THz refractive index of Si.<sup>11</sup> Consequently, the ratio of the amplitude spectrum of these waveguides is given by

$$A_w/A_{w0} = t_{12}t_{21} \exp[-(\alpha_1 n + \alpha_0 - \alpha_S)(20\ \text{mm})], \quad (1)$$

where  $A_w$  is the amplitude spectrum of the waveguide with the Si plate and  $A_{w0}$  is the amplitude spectrum of the waveguide without the Si. The parameter  $\alpha_1$  is the amplitude absorption coefficient of the parallel plate waveguide formed by the Al layers on the Si with the dielectric contribution removed, and  $\alpha_0$  is the amplitude absorption coefficient of the bare aluminum waveguide, which was determined by comparing bare Al waveguides of different lengths. The parameter  $\alpha_S$  is the small amplitude absorption coefficient of Si.<sup>11</sup> This expression is based on the fact that for the TEM mode of the parallel plate waveguide, the absorption coefficient for a dielectric (with index  $n$ ) filled waveguide is  $n$  times larger than for an air-filled waveguide.

The absorption coefficient  $\alpha_1$  decreased to  $\alpha_{1N}$  at liquid nitrogen temperature, which can be obtained from the ratio of the spectral amplitudes shown in Fig. 2 by the relationship

$$\frac{A_{wN}}{A_w} = \frac{\exp[-(n\alpha_{1N} + \alpha_{SN})(20\ \text{mm}) - \alpha_{0N}(10\ \text{mm})]}{\exp[-(n\alpha_1 + \alpha_S)(20\ \text{mm}) - \alpha_0(10\ \text{mm})]}. \quad (2)$$

Due to the narrowing of the Si phonon line responsible for the THz absorption at room temperature when the Si plate is cooled to 77 K, the THz absorption of Si is reduced

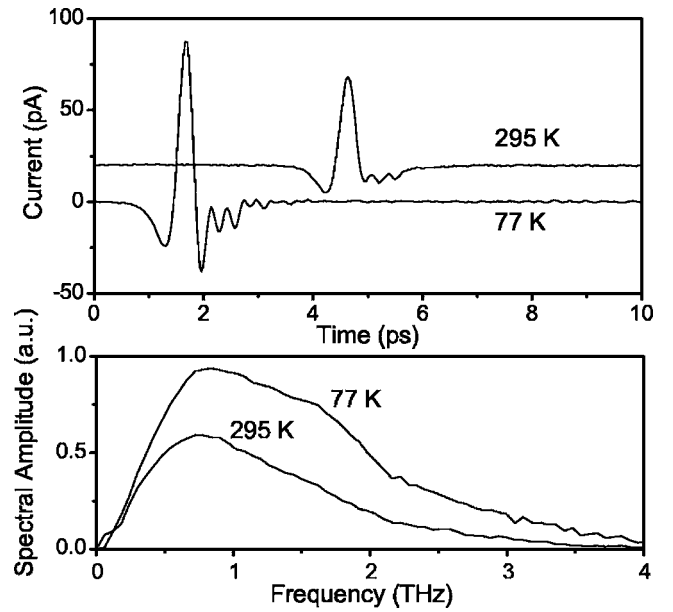


FIG. 2. Transmitted THz pulses through waveguide assembly of Fig. 1 and corresponding amplitude spectrum. THz pulse at 295 K is offset for clarity.

to an insignificant value, i.e.,  $\alpha_{SN} \ll \alpha_S$ . As explained earlier, the absorption of the bare Al plate waveguide does not change with cooling, i.e.,  $\alpha_{0N} \sim \alpha_0$ . Consequently, the above relationship can be simplified to

$$\frac{A_{wN}}{A_w} \approx \exp[-[(\alpha_{1N} - \alpha_1)n(20\ \text{mm}) - \alpha_S(20\ \text{mm})]], \quad (3)$$

from which  $\alpha_{1N}$  is evaluated as displayed in Fig. 3.

The theoretical absorption coefficient of an air-spaced parallel plate waveguide<sup>12</sup> is determined by  $\alpha_0 = R/(\eta_0 b)$ , where  $R = 10.88 \times 10^{-3} [10^7 / (\sigma_R \lambda_0)]^{0.5}$ ,  $\eta_0 = (\mu_0 / \epsilon_0)^{1/2} \approx 377\ \Omega$  is the free-space impedance,  $b$  is the gap between the plates,  $\sigma_R$  is the real part of the conductivity, and  $\lambda_0$  is the free-space wavelength. The frequency dependent metal conductivity  $\sigma$  can be modeled by the Drude formula

$$\sigma = \sigma_R + i\sigma_i = \sigma_{dc} i\Gamma / (\omega + i\Gamma) = i\epsilon_0 \omega_p^2 / (\omega + i\Gamma), \quad (4)$$

where  $\epsilon_0$  is the free-space permittivity,  $\omega$  is the angular frequency,  $\omega_p$  is the angular plasma frequency, and  $\Gamma$  is the electron scattering rate. The conductivity can be rewritten in the form

$$\sigma = \epsilon_0 \omega_p^2 / [\Gamma(1 + \omega^2/\Gamma^2)] + i\epsilon_0 \omega_p^2 \omega / [\Gamma^2(1 + \omega^2/\Gamma^2)]. \quad (5)$$

For the conditions of our experiment,  $\omega \ll \Gamma$  and to a good approximation  $\sigma_R \approx \epsilon_0 \omega_p^2 / \Gamma$ . For bulk Al at room temperature,  $\Gamma/2\pi = 19.4$  THz.<sup>13</sup> According to Matthiessen's rule,  $\Gamma = \Gamma_P + \Gamma_D$  is the sum of a temperature dependent term  $\Gamma_P$ , generally dominated by phonons at the experimental temperatures, and a temperature independent term  $\Gamma_D$ , generally dominated by lattice defects. The different absorption coefficients  $\alpha_0$ ,  $\alpha_{0N}$ ,  $\alpha_1$ , and  $\alpha_{1N}$  due to the different metal surfaces and temperatures correspond to the different scattering rates,  $\Gamma_0 = \Gamma_{0P} + \Gamma_{0D}$ ,  $\Gamma_1 = \Gamma_{1P} + \Gamma_{1D}$ , and  $\Gamma_{1N} = \Gamma_{1PN} + \Gamma_{1DN}$ .

Given the tabulated conductivity of bulk Al (Refs. 4 and 5) is  $\sigma_B = 3.8 \times 10^5\ \Omega^{-1}\ \text{cm}^{-1}$ , the experimental and theoretical absorption coefficients  $\alpha_1$  at room temperature match well, as shown in Fig. 3, indicating the high quality metal at the Al/Si interface. The reduction of the absorption coefficient

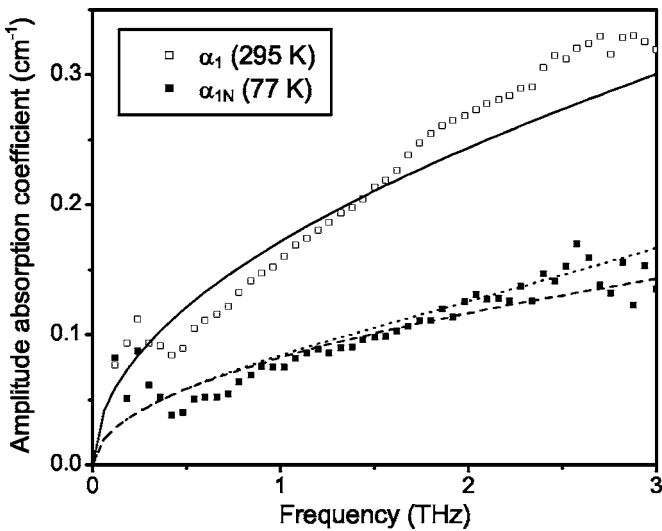


FIG. 3. Waveguide amplitude absorption coefficient  $\alpha_1$  of Al film on Si (Al/Si interface). Open squares are experimental results for  $\alpha_1$  at 295 K and solid squares correspond to  $\alpha_{1N}$  at 77 K. Lines are theoretical predictions, with the solid line calculated with the frequency independent conductivity  $\sigma_R = 3.8 \times 10^5 \Omega^{-1} \text{cm}^{-1}$ , the dashed line calculated with the frequency independent  $\sigma_R = 1.6 \times 10^6 \Omega^{-1} \text{cm}^{-1}$ , and the dotted line using the frequency dependent  $\sigma_R(\omega)$  of Eq. (5) with  $\sigma_R(0) = 1.6 \times 10^6 \Omega^{-1} \text{cm}^{-1}$  and  $\Gamma_{1N}/2\pi = 4.8 \text{ THz}$ .

cient  $\alpha_{1N}$  at 77 K corresponds to an increase in the conductivity of approximately 4, corresponding to a reduction of  $\Gamma$  by a factor of 1/4 (i.e.,  $\Gamma_{1N} = \Gamma_1/4$ ). This conductivity increase is substantially less than the well known increase of 8 for the bulk Al,<sup>4,5</sup> further illustrating the importance of lattice defects even for this high quality surface layer. For bulk Al at 77 K,  $\Gamma_{BDN} \ll \Gamma_{BPN}$ . In contrast, the scattering rate for the Al/Si interface at 77 K is approximately twice the value for bulk Al ( $\Gamma_{1N} \approx 2\Gamma_{BN}$ ), implying that  $\Gamma_{1DN}$  for this interface has increased such that  $\Gamma_{1DN} \sim \Gamma_{1PN}$ . For the other examined surfaces, there was no observed increase in conductivity, implying that  $\Gamma_D \gg \Gamma_P$  for all of the measured temperatures. This is consistent with our measured value of the absorption  $\alpha_0$  of the bare Al waveguide, which was approximately twice the value of  $\alpha_1$ , corresponding to  $\Gamma_0$  which is four times greater than both  $\Gamma_1$  for the Al/Si interface and  $\Gamma_B$  for bulk Al at 295 K.

Given the conductivity increase of the Al/Si interface,  $\Gamma_1$  has correspondingly decreased by a factor of 4 to approximately  $\Gamma_{1N}/2\pi \sim 5 \text{ THz}$  at 77 K,<sup>13</sup> implying that the frequency dependence of the conductivity  $\sigma_R$ , as shown in Eq. (5), plays only a minor role over the measured frequency

range. This is shown by the small difference between the frequency dependent and frequency independent theoretical predictions in Fig. 3. It is expected that for metals with higher dc conductivities, the frequency dependent conductivity will decrease significantly at measurable frequencies, limiting further reduction in absorption. This work with evaporated films can be extended to these metals with longer electron scattering times such as silver, which will allow the examination of the frequency dependence of the conductivity.

In summary, the conductivities at THz frequencies of a number of different Al and Cu plates were measured by waveguide THz-TDS, and were found not to increase when cooled from 295 to 77 K. This result was also found with the Al/air interface of Al films evaporated on Al, glass, and Si. The consequent reduced conductivity can be attributed to a large amount of carrier scattering due to lattice defects within the 100 nm THz skin-depth layer. However, the conductivity of the Al/Si interface of a 300 nm Al film deposited on a polished Si wafer was found to increase by approximately a factor of 4 when cooled from 295 to 77 K, illustrating the importance and fragility of the quality of the metal lattice.

The authors would like to thank S. Sree Harsha and Yuguang Zhao for their technical assistance, particularly in metalizing the 50  $\mu\text{m}$  Si wafer. This work was partially supported by the National Science Foundation.

- <sup>1</sup>G. Gallot, S. P. Jamison, R. W. McGowan, and D. Grischkowsky, *J. Opt. Soc. Am. B* **17**, 851 (2000).
- <sup>2</sup>R. Mendis and D. Grischkowsky, *Opt. Lett.* **26**, 846 (2001).
- <sup>3</sup>R. Mendis and D. Grischkowsky, *IEEE Microw. Wirel. Compon. Lett.* **11**, 444 (2001).
- <sup>4</sup>P. D. Desai, H. M. James, and C. Y. Ho, *J. Phys. Chem. Ref. Data* **13**, 1131 (1984).
- <sup>5</sup>*CRC Handbook of Chemistry and Physics*, 73rd ed. edited by D. R. Lide (CRC, Boca Raton, FL, 1993), pp. 12–34.
- <sup>6</sup>Jiangquan Zhang and D. Grischkowsky, *Opt. Lett.* **29**, 1031 (2004).
- <sup>7</sup>Joseph S. Melinger, N. Laman, S. Sree Harsha, and D. Grischkowsky, *Appl. Phys. Lett.* **89**, 251110 (2006).
- <sup>8</sup>Manuel Cardona, William Paul, and Harvey Brooks, *J. Phys. Chem. Solids* **8**, 204 (1959).
- <sup>9</sup>K. G. Lyon, G. L. Salinger, C. A. Swenson, and G. K. White, *J. Appl. Phys.* **48**, 865 (1977).
- <sup>10</sup>R. G. Chambers, *Proc. R. Soc. London, Ser. A* **215**, 481 (1952).
- <sup>11</sup>Jianming Dai, Jiangquan Zhang, Weili Zhang, and D. Grischkowsky, *J. Opt. Soc. Am. B* **21**, 1379 (2004).
- <sup>12</sup>N. Marcuvitz, *Waveguide Handbook* (Peter Peregrinus, London, 1993), pp. 21 and 65.
- <sup>13</sup>M. A. Ordal, L. L. Long, R. J. Bell, S. E. Bell, R. R. Bell, R. W. Alexander, Jr., and C. A. Ward, *Appl. Opt.* **22**, 1099 (1983).